



## Nitric oxide and nitroxyl formation in the reduction of *trans*-tetraamminenitrosyltriethylphosphiteruthenium(II) ion

Gustavo Metzker<sup>a</sup>, Eliane Vasconcelos Stefaneli<sup>a</sup>, José Clayston Melo Pereira<sup>a</sup>, Francisco das Chagas Alves Lima<sup>b</sup>, Sebastião Claudino da Silva<sup>c</sup>, Douglas Wagner Franco<sup>a,\*</sup>

<sup>a</sup>Instituto de Química de São Carlos, Universidade de São, 400 Trabalhador São Carlense ave, 13560-970 São Carlos, SP, Brazil

<sup>b</sup>Centro de Ciências da Natureza, Coordenação de Química, Universidade Estadual do Piauí, 2231 João Cabral St, 64002-150 Teresina, PI, Brazil

<sup>c</sup>Departamento de Química, Universidade Federal do Mato Grosso, 2367 Fernando Correia da Costa ave, 78060-900 Cuiabá, MT, Brazil

### ARTICLE INFO

#### Article history:

Received 6 January 2011

Received in revised form 27 September 2012

Accepted 29 September 2012

Available online 13 October 2012

#### Keywords:

Nitrosyl complexes

Nitric oxide

Nitroxyl

Europium

Zinc amalgam

### ABSTRACT

The reduction of *trans*-[Ru(NO)(NH<sub>3</sub>)<sub>4</sub>(P(OEt)<sub>3</sub>)<sub>3</sub>]<sup>3+</sup> ion was investigated in aqueous medium. Due to the phosphite ligand *trans*-effect and *trans*-influence, this complex selectively releases NO or HNO after one or two electrons reduction centered at the nitrosonium ligand (NO<sup>+</sup>). These reactions were carried out through electrochemical reduction and using Eu<sup>2+</sup> and zinc amalgam, and the products were identified using electrochemical and spectroscopic techniques. Only the reduction of the nitrosonium ligand to nitric oxide is observed when europium is used as reductant. When the reaction is carried out with Zn(Hg), nitric oxide formation was not observed and N<sub>2</sub>O, an indirect marker of HNO, is detected in solution.

© 2012 Elsevier B.V. All rights reserved.

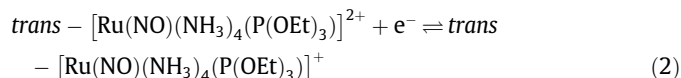
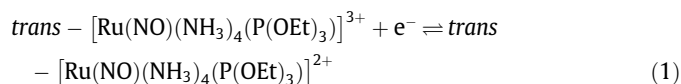
### 1. Introduction

Nitroxyl (HNO) is a highly reactive species that is attracting current attention due to its relationship to the sibling nitric oxide molecule (NO), regarding to its chemical properties and biological behavior [1–3]. The nitrosonium cation (NO<sup>+</sup>) and nitroxyl (HNO) have been suggested to be responsible for some functions ascribed to nitric oxide, such as vasodilatation and cytotoxicity [4,5]. Earlier studies suggest that HNO is an intermediate form of endothelium-derived relaxing factor, which led to the consideration of HNO as an alternative signaling agent to NO [6]. The difference between the physiological functions and cytotoxicities of NO and HNO was proposed to be mainly due to their reactivities toward proteins and enzymes containing iron center and thiols [3,7]. The Angeli's salt's (Na<sub>2</sub>N<sub>2</sub>O<sub>3</sub>) cytotoxicity was attributed to the chemical depletion of cellular glutathione (GSH) thus suggesting that HNO can affect the cysteine protease's activity by direct interaction with GSH [5].

Compounds that are able to release NO and HNO on a controlled way are desirable to modulate the local concentration of NO and HNO in the organism [3,8–12]. Among the series of NO donors, organic compounds, metal–NO complexes, nitrosothiols and enzyme-activated NO donors have received attention [8–10]. Unlike NO-donors, HNO donors has a restrict number of examples [3,11,12]. Among then,

Angeli's salt, Pilotys' salt, cyanamide, isopropylamine NONOate and acyloxy nitroso compounds have been investigated [11,12]. These compounds have some limitations like short half-life, concomitant NO liberation and in some cases toxic reaction co-products [11]. The sodium nitroprusside, a well recognized NO donor, also liberates HNO but in very special conditions [13].

The *trans*-[Ru(NO)(NH<sub>3</sub>)<sub>4</sub>(P(OEt)<sub>3</sub>)<sub>3</sub>]<sup>3+</sup> ion exhibits low cytotoxicity against host cells (LD<sub>50</sub> = 125 μmol/kg and IC<sub>50</sub> = 2.260 μM against Swiss mice and V-79 host cells, respectively) [14] and *k*<sub>NO</sub> (0.98 s<sup>-1</sup>) and *E*<sup>0</sup><sub>(NO<sup>+</sup>/NO<sup>0</sup>)</sub> = 0.04 V versus NHE values [15], which would make it a promising NO-donor model for pharmaceutical purposes [16,17]. Furthermore, this complex also presents a second well-defined one-electron reduction process at biologically accessible potentials, which was tentatively assigned to the reduction of the coordinated NO<sup>0</sup> [14,15]. In addition this compound exhibits like the other ruthenium tetraammine complexes, anti-parasitic action, ascribed to their nitric oxide and nitroxyl release capacity when reduced by one or two-electrons as exemplified in Eqs. (1) and (2) [16].



\* Corresponding author. Tel.: +55 16 3373 9970; fax: +55 16 3373 9976.

E-mail address: douglas@iqsc.usp.br (D.W. Franco).

Aiming to learn more about this system, the electrochemical behavior of  $trans\text{-}[\text{Ru}(\text{NO})(\text{NH}_3)_4(\text{P}(\text{OEt})_3)]^{3+}$  and its chemical reduction were investigated.

## 2. Experimental section

### 2.1. Chemicals and reagents

All chemicals, unless otherwise indicated, were of analytical grade and purchased from Sigma–Aldrich, Strem or Merck. Ruthenium trichloride was the starting material for the synthesis of all ruthenium complexes described herein. Zinc–amalgam was prepared by treating metallic zinc with a saturated solution of mercury(II) chloride in a  $5 \times 10^{-2}$  M solution of  $\text{HClO}_4$ . After 5 min, the amalgam was exhaustively washed with distilled water and immediately used.  $\text{Eu}^{2+}$  solution was prepared dissolving the desired amount of  $\text{Eu}_2\text{O}_3$  (99.99%) in an exhaustively deaerated acidic solutions in presence of  $\text{Zn}(\text{Hg})$ . After 20 min the reduction of  $\text{Eu}^{3+}$  to  $\text{Eu}^{2+}$  took place, and the solution was used immediately. All solvents were purified following known procedures [18]. Doubly distilled water was used throughout. All syntheses and manipulations were carried out under an argon atmosphere [19].

### 2.2. Synthesis of the complexes

$[\text{Ru}(\text{NH}_3)_5(\text{Cl})]\text{Cl}_2$  [20] and  $trans\text{-}[\text{Ru}(\text{NO})(\text{NH}_3)_4(\text{P}(\text{OEt})_3)](\text{PF}_6)_3$  were prepared and characterized as described in the literature [21].

### 2.3. Instruments

UV–Vis measurements were performed in a 1.00 cm quartz cell on a Hitachi U3501 spectrophotometer. Cyclic and differential pulse voltammetry experiments were performed with a PAR model 173 or 264 A potentiostat/galvanostat, coupled with a model 175 universal programmer. The three-electrode system, saturated calomel, glassy carbon and platinum wire were used as reference, work and auxiliary electrodes respectively. The potential values were converted and reported as normal hydrogen electrode (NHE). The  $^{31}\text{P}$  NMR spectrum was measured in  $\text{D}_2\text{O}$  solution at pH 3.0 (trifluoroacetic acid) using  $\text{PF}_6^-$  as the internal standard and recorded on a Bruker AC-200 spectrophotometer.

The NO detection was performed using a selective NO electrode (amino 700) from Innovative Instruments Inc. The electrode was polarized in water during 12 h before use. A GE Sievers 280i Nitric Oxide Analyser (NOA) was used to quantify the liberated NO. Aliquots of a stock solution of sodium nitrite were injected in the reaction vessel, constantly purged by inert gas (nitrogen), containing a solution of potassium iodide and glacial acetic acid. The area of the peaks was used to construct the calibration curve following manufacturer and literature recommendations [22]. Zinc analysis was carried out using a Varian 240 FS atomic absorption spectrometer.

### 2.4. Measurements

All manipulations were carried out in the absence of oxygen and the temperature was always maintained at  $T = (25 \pm 0.2)^\circ\text{C}$ , except when mentioned. The solution pH was kept below 5.0 during the experiments to avoid the nucleophilic attack of hydroxyl ions on the  $\text{NO}^+$  and  $\text{P}(\text{OEt})_3$  ligands [23]. All experiments, except when mentioned, were carried out at pH 4.2 ( $\text{CH}_3\text{COOH}/\text{CH}_3\text{COONa}$ ),  $\mu = 0.10$  M, ( $\text{CF}_3\text{COOH}/\text{CF}_3\text{COONa}$ ).

$\text{N}_2\text{O}$  saturated solution was obtained bubbling the gas (99.5%) directly in a pH 4.2 solution at  $(2.5 \pm 0.2)^\circ\text{C}$  during 30 min.

The inert gas (argon or nitrogen with high purity 99.999%) was deoxygenated by passing through a  $\text{Cr}(\text{II})$  solution prior to use [19]. The complex was stored under vacuum and protected from light and humidity and was used within 30 days. UV–Vis and NMR spectra of the solutions containing air-sensitive complexes were obtained under argon atmosphere. Using the inert gas pressure the solutions were transferred through Teflon tubing to a specific tube or cell. For zinc analysis, a calibration curve was prepared using a commercial standard zinc solution (1000 mg/L of Zn in  $\text{HNO}_3$  2% water solution). For samples analysis, the solid  $\text{Zn}(\text{Hg})$  was first separated by decantation from the resulting solution of the reaction between  $trans\text{-}[\text{Ru}(\text{NO})(\text{NH}_3)_4(\text{P}(\text{OEt})_3)]^{3+}$  and  $\text{Zn}(\text{Hg})$ . The liquid was quantitatively transferred to a 50 ml volumetric flask. The solid was washed with three portions of 3 ml of trifluoroacetic acid  $5 \times 10^{-4}$  M. These 9 ml were quantitatively transferred to the 50 ml volumetric flask. The volume was adjusted to the mark with trifluoroacetic solution and aliquots taken for the analysis.

### 2.5. Data treatment

The number of electrons for the  $[\text{RuNO}]^{2+}/[\text{RuNO}]^+$  process were calculated using the Lovric equation [23]:

$$\frac{\delta E_p}{\delta \log(f)} = \frac{-2.3RT}{\alpha nF} \quad (3)$$

where  $R$  is the gas constant,  $T$  is temperature,  $\alpha$  is the electron transfer coefficient,  $n$  is the number of electrons involved in electron transfer,  $F$  is the Faraday constant and  $f$  is frequency (range from 100 to 600 Hz). The reversibility check of the process and  $\alpha$  and  $n$  value calculations ( $2.5$  and  $25^\circ\text{C}$ ) were carried out using peak potential ( $E_p$ ) versus  $\log(f)$  plots [24].

### 2.6. Computational details

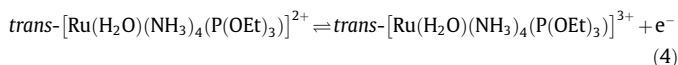
The quantum mechanical calculations were performed using the GAUSSIAN 03 package [25]. The molecular geometry optimizations were performed using the Kohn–Sham density functional theory (DFT) [26] with the Becke three-parameters hybrid exchange–correlation function, known as B3LYP [27,28]. The molecule was separated in two groups: (a) The  $\text{NO}\text{--}\text{Ru}\text{--}\text{P}(\text{O}\text{--})_3$  “bone” and (b) the  $\text{NH}_3$  and  $(\text{--CH}_2\text{CH}_3)$  fragments. In the first group there was used Dgauss basis DGDZVP for Ru and TGTZVP [29–31] for N, O, P and H. In the second group the Pople basis 3-21G was used. The natural bond orbital calculations were performed using the NBO 3.0 program [30–32], as implemented in the GAUSSIAN 03 package. For the DFT calculations, the  $(\text{NO})\text{--}\text{Ru}\text{--}\text{P}(\text{OEt})_3$  vector is defined as the  $z$  axis, and the  $x$  and  $y$  axis correspond to the  $\text{H}_3\text{N}\text{--}\text{Ru}\text{--}\text{NH}_3$  vectors.

To account for solvent effects of water, all the calculations were carried out using the polarizable continuum model (PCM) [33–35].

## 3. Results and discussion

### 3.1. Electrochemical reduction

The typical cyclic voltammogram for the  $trans\text{-}[\text{Ru}(\text{NO})(\text{NH}_3)_4(\text{P}(\text{OEt})_3)]^{3+}$  ion in aqueous acidic solution is shown in Fig. 1. In this Figure, a defined cathodic peak ( $E_{cp1}$ ) at 0.04 V coupled to an anodic peak ( $E_{ap1}$ ) at 0.11 V ascribed to the  $[\text{RuNO}]^{3+}/[\text{RuNO}]^{2+}$  process and a cathodic peak ( $E_{cp3}$ ) at 0.65 V coupled to an anodic peak ( $E_{ap3}$ ) at 0.80 V due to the  $[\text{RuH}_2\text{O}]^{3+}/[\text{RuH}_2\text{O}]^{2+}$  process can be observed Eqs. (1) and (4).



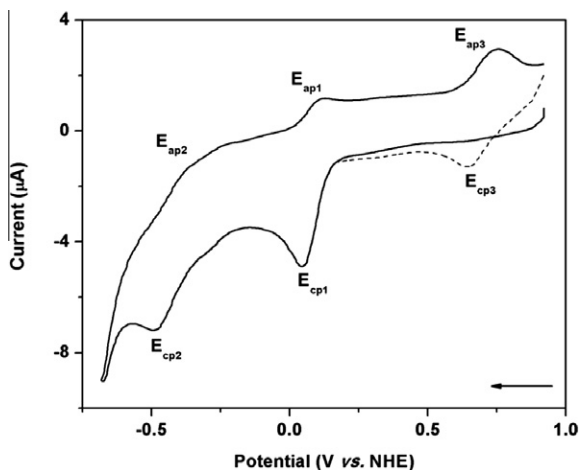
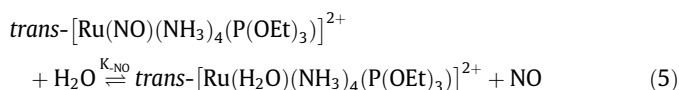


**Fig. 1.** Cyclic voltammogram for the  $trans\text{-}[\text{Ru}(\text{NO})(\text{NH}_3)_4(\text{P}(\text{OEt})_3)]^{3+}$  ion in aqueous solution: pH 4.2;  $\mu = 0.10 \text{ M}$ ;  $T = (2.5 \pm 0.2)^\circ\text{C}$ ;  $C_{\text{Ru}} = 1.2 \times 10^{-3} \text{ M}$ ; scan rate =  $100 \text{ mV/s}$ . Solid line: first cycle; dashed line: second cycle.

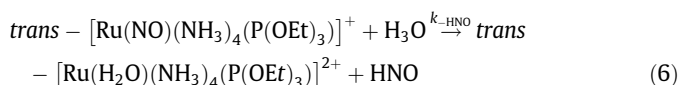
The dependence of the anodic peak ( $E_{\text{ap1}}$ ) current with the scan rate and temperature was due to the fast dissociation of NO ( $k_{-\text{NO}} = 0.98 \text{ s}^{-1}$ , Eq. (5)) [21].



Furthermore, in Fig. 1, a third process is observed ( $E_{\text{cp2}}$ ) at  $-0.46 \text{ V}$ , in which the anodic counterpart ( $E_{\text{ap2}}$ ) is barely noticeable on the  $-0.30$  to  $-0.35 \text{ V}$  region.

The comparison among of the cathodic peak currents that correspond to processes  $E_{\text{cp1}}$  and  $E_{\text{cp2}}$ , after the deconvolution of the square wave polarograms (Fig. S1, Supplementary material) strongly suggesting the one-electron nature of  $E_{\text{cp2}}$ . The plot of peak potential ( $E_{\text{cp}}$ ) versus  $\log(f)$  was linear, as expected [23] for an irreversible process. The values for  $\alpha$  and  $n$ , calculated from the plots at  $2.5$  and  $25^\circ\text{C}$ , are  $0.5$  and  $0.98$ , respectively, as expected for a one-electron process.

The process at  $E_{\text{cp3}}$  was tentatively assigned to the  $[\text{RuNO}]^{2+}/[\text{RuNO}]^+$  couple Eq. (2). This process, although electrochemically reversible, is chemically irreversible due to both the low stability of the ruthenium nitroxyl bond and the fast aquation of the nitroxyl ligand as a consequence of the strong  $\text{P}(\text{OEt})_3$  ligand *trans* effect and *trans* influence. It was observed that the ratios  $i_{\text{ap1}}/i_{\text{cp1}}$  and  $i_{\text{ap2}}/i_{\text{cp2}}$  increased with the scan rate, indicating that the second reduction is dependent on the corresponding  $[\text{RuNO}]^{3+}/[\text{RuNO}]^{2+}$  process. This hypothesis was also supported by the experiments at  $2.5^\circ\text{C}$ , and using scan rates faster than  $1 \text{ V/s}$  in which the  $[\text{RuNO}]^{3+}/[\text{RuNO}]^{2+}$  process became reversible, since the current of the process  $E_{\text{ap1}}$  increased due to the decrease of the rate for the NO dissociation as a consequence of the temperature [21]. These results suggest that the behavior of  $E_{\text{cp2}}$  would be coherent with Eq. (6):



No direct measurements have been carried out for  $k_{-\text{HNO}}$  determination. However a comparison between the  $i_{\text{ap1}}/i_{\text{cp1}}$  and  $i_{\text{ap2}}/i_{\text{cp2}}$  (Fig. 1) ratios as a function of the temperature and scan rates suggests that  $k_{-\text{HNO}} \geq k_{-\text{NO}}$ .

The DFT-MO calculation showed that the LUMO ( $\text{Ru } d_{xz}$  36%;  $\text{NO } p_{\pi^*}$  63%) and LUMO+1 ( $\text{Ru } d_{xy}$  35%;  $\text{NO } p_{\pi^*}$  65%) of the nitrosonium complex  $[\text{RuNO}]^{3+}$  are antibonding orbitals and that the one-electron reduction would be more localized on the  $\text{NO}^+$  ligand, which

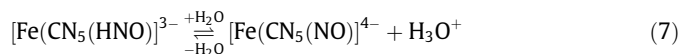
is in agreement with previous results [14,15]. The calculations also showed that the second electron reduction also occurs on the nitric oxide ligand because the LUMO of the  $trans\text{-}[\text{Ru}(\text{NO})(\text{NH}_3)_4(\text{P}(\text{OEt})_3)]^{2+}$  ion is predominantly a  $\pi$ -antibonding orbital and is more localized on the NO ligand ( $\text{Ru } d_{xz}$  16%;  $\text{NO } \pi^*$  80%).

DFT calculations for both singlet and triplet multiplicities for  $\text{NO}^-$  and  $\text{HNO}$ , uncoordinated and coordinated to ruthenium moiety in aqueous solution were considered. Regarding to the non-protonated species, the uncoordinated  $^3\text{NO}^-$  is more stable than the  $^1\text{NO}^-$  by  $30 \text{ kcal/mol}$ . When  $\text{NO}^-$  is coordinated, the global energy of  $trans\text{-}[\text{Ru}(\text{NO})(\text{NH}_3)_4(\text{P}(\text{OEt})_3)]^+$ , triplet and singlet forms, are similar being the singlet  $0.8 \text{ kcal/mol}$  more stable than the triplet one. Considering the energy difference between the uncoordinated and coordinated  $\text{NO}^-$ , the bonding to the fragment  $[\text{Ru}(\text{NH}_3)_4(\text{P}(\text{OEt})_3)]$  stabilizes the singlet structure by  $31 \text{ kcal/mol}$ .

Similar behavior was found for uncoordinated and coordinated HNO. For the uncoordinated species,  $^1\text{HNO}$  is more stable than the  $^3\text{HNO}$  by  $8 \text{ kcal/mol}$ . However, when coordinated the stabilization energy difference grown up to  $40 \text{ kcal/mol}$ . Once again the  $^1\text{HNO}$  is more stable regarding to the  $^3\text{HNO}$  by  $32 \text{ kcal/mol}$ .

Thus, the DFT calculations indicate that for the nitroxyl species, protonated or not, the singlet structure is favorable respecting to the triplet one. This also can be observed comparing the calculated bond order for the Ru–N bond:  $1.23$  ( $^1\text{NO}^-$ );  $0.622$  ( $^3\text{NO}^-$ );  $0.943$  ( $^1\text{HNO}$ ) and  $0.435$  ( $^3\text{HNO}$ ). As expected, the calculated Ru–N–O angles are:  $120.1^\circ$  ( $^1\text{NO}^-$ );  $126.1^\circ$  ( $^3\text{NO}^-$ );  $127.2^\circ$  ( $^1\text{HNO}$ ) and  $119.6^\circ$  ( $^3\text{HNO}$ ). These values are coherent with the ones reported for ruthenium complex containing  $\text{NO}^-$  as ligand [36] and as expected are lower than the calculated values for  $[\text{Ru}(\text{N}=\text{O})^*]$ :  $176.1^\circ$  ( $\text{NO}^+$ ) and  $134.4^\circ$  ( $\text{NO}^0$ ). The dissociation energy ( $\text{kcal/mol}$ ) of  $\text{NO}^-$  and HNO from the metal center follows similar trend:  $36.1$  ( $^1\text{NO}^-$ );  $14.2$  ( $^3\text{NO}^-$ );  $19.9$  ( $^1\text{HNO}$ ) and  $4.2$  ( $^3\text{HNO}$ ). More DFT calculated parameters can be found at Supplementary material (Table S1).

The  $\text{pK}_a$  value for the HNO molecule is reported to be higher than  $11.0$  [37,38]. However, an increase of acidity is reported to occur when HNO is coordinated to a metal center [37]. This is the case of  $[\text{Fe}(\text{CN})_5(\text{HNO})]^{3-}$  for a  $\text{pK}_a$  value of  $7.7$  Eq. (7) was measured [13].



Therefore it was likely that  $trans\text{-}[\text{Ru}(\text{HNO})(\text{NH}_3)_4(\text{P}(\text{OEt})_3)]^{2+}$  would exhibit an  $\text{pK}_a$  value smaller than  $11$ , coherently with the fact that backbonding effects are not operative in the Ru–HNO bond and therefore the  $\sigma$  inductive effect predominates along the Ru–N axial bond. DFT calculation for the  $\text{pK}_a$  [39,40] of the singlet form leads to the value of  $9.9$ . Since the singlet form is more stable than the triplet one, it would be reasonable that the nitroxyl complex in the conditions of the experiments ( $\text{pH} < 5.0$ ), would be as  $trans\text{-}[\text{Ru}(\text{HNO})(\text{NH}_3)_4(\text{P}(\text{OEt})_3)]^{2+}$ . According to DFT calculations, since there is not spin-restriction, the proton equilibrium between the coordinated singlet species is expected to be fast as usual. This is not the case for the uncoordinated ligand where, being the triplet form ( $^3\text{NO}^-$ ) more stable, the protonation ( $^1\text{HNO}$ ) is spin-restricted [1,38].

### 3.2. Release of NO and HNO from the $trans\text{-}[\text{Ru}(\text{NO})(\text{NH}_3)_4(\text{P}(\text{OEt})_3)]^{3+}$ ion upon chemical reduction

The reaction between  $trans\text{-}[\text{Ru}(\text{NO})(\text{NH}_3)_4(\text{P}(\text{OEt})_3)]^{3+}$  and  $\text{Eu}^{2+}$  was carried out using  $0.5$ ,  $1$ ,  $2$  and  $10$  equivalents of  $\text{Eu}^{2+}$  in acidic medium and the NO liberated identified using selective NO electrode (Fig. S2, Supplementary material) and quantified by NOA. Since the formal potential for  $\text{Eu}^{3+/2+}$  ( $E^0 = -0.55 \text{ V}$ ) [41] is thermodynamically favorable to promote the reduction of coordinated  $\text{NO}^0$  to  $\text{NO}^-$  ( $E_{\text{cp2}} = -0.46 \text{ V}$ ) it would be expected that the addition

of two equivalents of  $\text{Eu}^{2+}$  would diminish the amount of NO liberated if part of it would be reduced to nitroxyl. This was not observed (1, 2 and 10  $\text{Eu}^{2+}$  equivalents). The same concentration of NO was produced in the experiments as judged by the peaks area corresponding to NO in NOA and it was almost quantitative regarding to the initial amount of  $\text{trans}[\text{Ru}(\text{NO})(\text{NH}_3)_4(\text{P}(\text{OEt})_3)_3]^{3+}$  (Table S2). Also, cyclic and differential pulse voltammograms of the solutions after the addition of  $\text{Eu}^{2+}$  did not indicate the presence of the peak corresponding to  $\text{N}_2\text{O}$  at  $-0.32$  V (see discussion below). The final complex was identified and quantified as  $\text{trans}[\text{Ru}(\text{H}_2\text{O})(\text{NH}_3)_4(\text{P}(\text{OEt})_3)_2]^{2+}$  by its CV, UV–Vis and  $^{31}\text{P}$  NMR spectra [21].

The stepwise reduction of coordinated nitrosyl in  $[\text{Fe}(\text{CN})_5\text{NO}]^{2-}$  to NO and HNO is described [13] to occur when one and two equivalents of  $\text{Na}_2\text{S}_2\text{O}_4$  were respectively added into the metal complex solution. However, conversely to the described for  $[\text{Fe}(\text{CN})_5\text{NO}]^{2-}$  dithionite only leads to NO liberation from  $\text{trans}[\text{Ru}(\text{NO})(\text{NH}_3)_4(\text{P}(\text{OEt})_3)_3]^{3+}$  even when used in excess (3 equivalents), thus suggesting that in the last case reduction to nitroxyl does not occurs. This reaction is under investigation in this Laboratory.

The reduction on the  $\text{trans}[\text{Ru}(\text{NO})(\text{NH}_3)_4(\text{P}(\text{OEt})_3)_3]^{3+}$  ion was than investigated using  $\text{Zn}(\text{Hg})$ ,  $E^0 = -1.1$  V Eq. (8) [41].



On the present system the medium do not contains any special ligand to stabilize the low oxidation state of zinc and assuming that the electron transfer would occurs stepwise, the rate for the second electron ( $k_2$ ) transfer from the  $\text{Zn}^+$  or  $\text{Zn}_2^{2+}$  to the *in situ* generated  $\text{trans}[\text{Ru}(\text{NO})(\text{NH}_3)_4(\text{P}(\text{OEt})_3)_2]^{2+}$  would be faster or at least similar to the first one [42,43].

When  $\text{Zn}(\text{Hg})$  is used as reductant, nitric oxide evolution, the expected product of one electron transfer to  $\text{trans}[\text{Ru}(\text{NO})(\text{NH}_3)_4(\text{P}(\text{OEt})_3)_3]^{3+}$  was not noticed in the chronoamperogram. However, after 60 min of reaction, UV–Vis spectrum of this solution showed only the presence of the complex  $\text{trans}[\text{Ru}(\text{H}_2\text{O})(\text{NH}_3)_4(\text{P}(\text{OEt})_3)_2]^{2+}$ .

As observed in Fig. 2 the differential pulse voltammograms of solutions containing  $\text{trans}[\text{Ru}(\text{NO})(\text{NH}_3)_4(\text{P}(\text{OEt})_3)_3]^{3+}$  clearly show the  $[\text{RuNO}]^{3+}/[\text{RuNO}]^{2+}$  (Fig. 2A) and the  $[\text{RuNO}]^{2+}/[\text{RuNO}]^+$  process (Fig. 2B). Few minutes after the addition of  $\text{Zn}(\text{Hg})$  into this solution the intensities of the peaks corresponding to both process decreased and a new irreversible process (Fig. 2C) was observed at  $E_{\text{cp}} = -0.32$  V.

If HNO is formed it is expected do dimerize to  $\text{N}_2\text{O}$  ( $k_{\text{dim}} = 8 \times 10^6 \text{ M}^{-1} \text{ s}^{-1}$ ) [38]. Since a direct proof for HNO presence is not easily accessible,  $\text{N}_2\text{O}$  identification is used as an indirect proof of nitroxyl formation (Eq. (9)) [3,11]. Thus, a saturated  $\text{N}_2\text{O}$  solution was examined and found to display a comparable electrochemical behavior, thus allowing the tentative assignment:



The cyclic and differential pulse voltammetric experiments carried out using a  $\text{N}_2\text{O}$  saturated solution clearly showed a cathodic process at  $-0.32$  V (Fig. 2C) [44] which features are similar to the ones observed for the solution containing  $\text{trans}[\text{Ru}(\text{NO})(\text{NH}_3)_4(\text{P}(\text{OEt})_3)_3]^{3+}$  and  $\text{Zn}(\text{Hg})$  under the same experimental conditions (Fig. 2).

The electrochemical reduction of  $\text{N}_2\text{O}$  is pH dependent and is also influenced by the electrode composition [44] nevertheless this comparison, despite being only qualitative, corroborate with the above attribution.

Upon adding  $\text{Zn}(\text{Hg})$  into solutions containing the  $\text{trans}[\text{Ru}(\text{NO})(\text{NH}_3)_4(\text{P}(\text{OEt})_3)_3]^{3+}$  ion ( $\lambda = 316$  nm,  $\epsilon = 216 \text{ M}^{-1} \text{ cm}^{-1}$ ) [45] an increase of absorbance at 316 nm was observed reaching a maximum value in a period of one hour (Fig. 3). An isosbestic

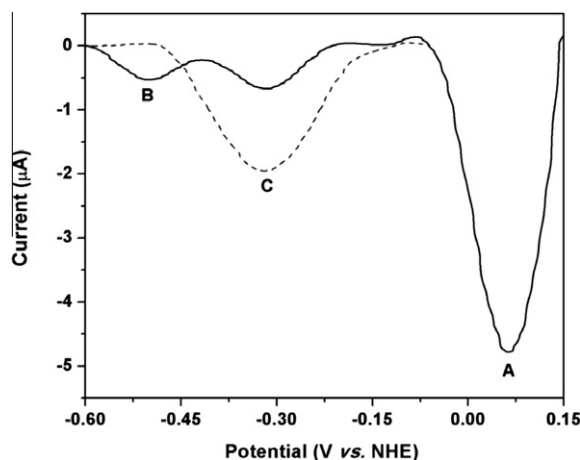


Fig. 2. Differential pulse voltammograms of the reaction between  $\text{trans}[\text{Ru}(\text{NO})(\text{NH}_3)_4(\text{P}(\text{OEt})_3)_3]^{3+}$  and  $\text{Zn}(\text{Hg})$ . Solid line: DPV after 30 min of reaction; Dashed line: DPV of a  $\text{N}_2\text{O}$  saturated solution.  $C_{\text{Ru}} = 5.0 \times 10^{-3} \text{ M}$ ; pH 4.2;  $\mu = 0.10 \text{ M}$ ; scan rate = 10 mV/s; pulse height = 50 mV;  $T = (2.5 \pm 0.2) ^\circ\text{C}$ .

point is observed at  $\lambda = 285$  nm. This spectral change was ascribed to the  $\text{trans}[\text{Ru}(\text{H}_2\text{O})(\text{NH}_3)_4(\text{P}(\text{OEt})_3)_2]^{2+}$  ion formation ( $\lambda = 316$  nm and  $\epsilon = 650 \text{ M}^{-1} \text{ cm}^{-1}$ ) [45]. The  $\text{trans}[\text{Ru}(\text{H}_2\text{O})(\text{NH}_3)_4(\text{P}(\text{OEt})_3)_2]^{2+}$  ion was also confirmed through the signal at 148 ppm in the  $^{31}\text{P}$  NMR spectrum [21,45] and quantified using pyrazine, which reacts with this aquo complex, yielding the  $\text{trans}[\text{Ru}(\text{NH}_3)_4(\text{P}(\text{OEt})_3)_2(-\text{pz})]^{2+}$  species ( $\lambda = 366$  nm,  $\epsilon = 4.2 \times 10^3 \text{ M}^{-1} \text{ cm}^{-1}$ ) [21]. The nitrosyl complex is quantitatively converted into the aquo species. The quantification of  $\text{Zn}^{2+}$  in solution after the reduction was over, indicates the presence of one equivalent (indeed  $1.05 \pm 0.06$ ) of  $\text{Zn}^{2+}$  per initial  $\text{trans}[\text{Ru}(\text{NO})(\text{NH}_3)_4(\text{P}(\text{OEt})_3)_3]^{3+}$  ion. It is interesting to point out that very little amount of  $\text{Zn}^{2+}$  (less than 5% of the expected if one electron reduction takes place) was found in a saturated NO solution, after 30 min of standing in presence of  $\text{Zn}(\text{Hg})$ .

Although no direct HNO analysis was carried out, taking in account the electrochemical, spectroscopic data and the reaction products analysis, it is likely to suppose that the reaction below Eq. (10) would be taking place:

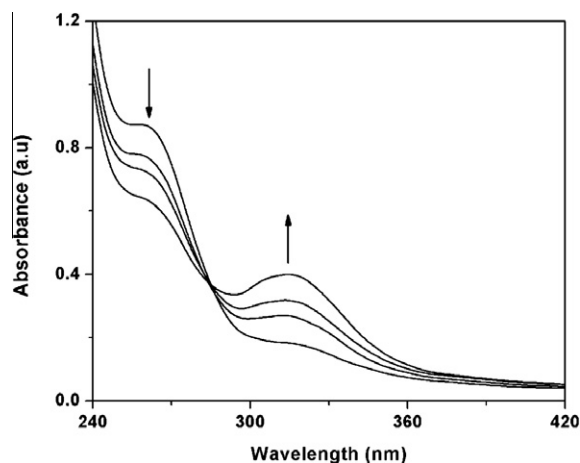
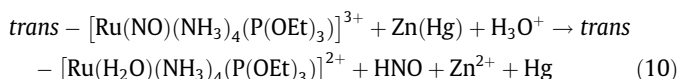


Fig. 3. Spectral change during the reaction between  $\text{trans}[\text{Ru}(\text{NO})(\text{NH}_3)_4(\text{P}(\text{OEt})_3)_3]^{3+}$  and  $\text{Zn}(\text{Hg})$ .  $C_{\text{Ru}} = 5.0 \times 10^{-4} \text{ M}$ ; pH 4.2;  $\mu = 0.10 \text{ M}$ ;  $T = (2.5 \pm 0.2) ^\circ\text{C}$ . One hour of reaction.

As observed above, taking in account the results obtained with  $\text{Eu}^{2+}$ ,  $\text{S}_2\text{O}_4^{2-}$  and  $\text{Zn}(\text{Hg})$ , the reductant potential is a necessary but not sufficient condition for the nitroxyl formation. The intrinsic reaction mechanism would be relevant to define the products of the reaction. This is the case for the reaction between ruthenium nitrosyl complexes and cysteine, a one electron reductant, [46] for which was postulated the formation of an adduct containing two cysteine molecules and one ruthenium nitrosyl complex, yielding HNO as a final product. This subject is under investigation at our Laboratory.

There are reports in the literature [36,47] of bonded  $\text{NO}^-$  to ruthenium complexes. The complex  $[\text{RuCl}(\text{NO})_2(\text{P}(\text{C}_6\text{H}_5)_3)_2]^+$  exhibit a well documented example of fluxional interchange between  $\text{NO}^-$  and  $\text{NO}^+$  ligands; and the complex  $[\text{Ru}(\text{NO})\text{Hedta}]^{2-}$  interesting example of coordinated singlet  $\text{NO}^-$ . However these compounds are usually robust. Kinetic data on nitroxyl dissociation and examples of inorganic HNO donors, besides the Angeli's Salt are not abundant [1,3,12]. The formation of  $[\text{Fe}(\text{CN})_5\text{HNO}]^{3-}$  with the subsequent HNO liberation is described to occur, but only in presence of excess of  $\text{CN}^-$  to retard the *trans* cyanide ion dissociation [13].

Recently was reported the electrochemical reduction of the nitric oxide ligand in *cis*- $[\text{Ru}(\text{NO})(\text{Cl})_2(\text{dppp})(\text{py})]\text{PF}_6$  without change in the coordination sphere [48]. The interpretation of this process at more negative potentials than the one attributed for the  $[\text{RuNO}]^{3+}/[\text{RuNO}]^{2+}$  couple was attributed to the formation of the nitroxyl ligand. However, since no strong *trans* labilizing ligand are present in the coordination sphere, the nitroxyl ligand remains coordinated to the metal center, which would limit these compounds eventual applications as a HNO donors.

It is likely the ability to generate NO and HNO upon controlled reduction, described for *trans*- $[\text{Ru}(\text{NO})(\text{NH}_3)_4(\text{P}(\text{OEt})_3)_3]^{3+}$  would be also observed for the other phosphite complexes of the series where  $\text{P}(\text{III}) = \text{P}(\text{OR})_3$ ,  $\text{P}(\text{OR})_2(\text{OH})$  and  $\text{P}(\text{OH})_3$ , all strong *trans* labilizing ligands. The present findings are an additional incentive for tailoring phosphite nitrosyl complexes more resistant to nucleophilic attack [23,49] and therefore more stable in a wide range of pH. This subject is now under investigation and results will be reported later.

#### 4. Conclusion

According to the experimental data, *trans*- $[\text{Ru}(\text{NO})(\text{NH}_3)_4(\text{P}(\text{OEt})_3)_3]^{3+}$  ion behaves as a fast NO and or HNO donor, which could be selectivity tuned through the judicious choice of the electrochemical potential or the chemical reductant.

#### Acknowledgments

The authors acknowledge the Brazilian agencies FAPESP, CAPES and CNPq for their financial support. The authors also thank A.N. Chiba and Professor E. Tfouni (FFCLRP-USP) for the NOA measurements.

#### Appendix A. Supplementary material

Supplementary data associated with this article can be found, in the online version, at <http://dx.doi.org/10.1016/j.ica.2012.09.042>.

#### References

- [1] J.M. Fukuto, C.H. Switzer, K.M. Miranda, D.A. Wink, Annu. Rev. Pharmacol. Toxicol. 45 (2005) 335.
- [2] C.H. Switzer, W. Flores-Santana, D. Mancardi, S. Donzelli, D. Basudhar, L.A. Ridnour, K.M. Miranda, J.M. Fukuto, N. Paolucci, D.A. Wink, Biochim. Biophys. Acta 1787 (2009) 835.
- [3] K.M. Miranda, Coord. Chem. Rev. 249 (2005) 433.
- [4] D.A. Wink, M. Feelisch, J.M. Fukuto, D. Chistodoulou, D. Jourdeuil, M.B. Grisham, Y. Vodovotz, J.A. Cook, M. Krishna, W.G. DeGraff, S. Kim, J. Gamson, J.B. Mitchell, Arch. Biochem. Biophys. 351 (1998) 66.
- [5] J.M. Fukuto, A.J. Hobbs, L.J. Ignarro, Biochem. Biophys. Res. Commun. 196 (1993) 707.
- [6] J.M. Fukuto, K. Chiang, R. Hsieh, P. Wong, G. Chaudhuri, J. Pharmacol. Exp. Ther. 263 (1992) 546.
- [7] P.C. Ford, I.M. Lorkovic, Chem. Rev. 102 (2002) 993.
- [8] P.G. Wang, T.B. Cai, N. Taniguchi (Eds.), Nitric Oxide Donors For Pharmaceutical and Biological Applications, Wiley-VCH, Weinheim, 2005.
- [9] P.G. Wang, M. Xian, X. Tang, X. Wu, Z. Wen, T. Cai, A.J. Janczuk, Chem. Rev. 102 (2002) 1091.
- [10] M.R. Miller, I.L. Megson, Br. J. Pharmacol. 151 (2007) 305.
- [11] J.C. Irvine, R.H. Ritchie, J.L. Favaloro, K.L. Andrews, R.E. Widdop, B.K. Kemp-Harper, Trends Pharmacol. Sci. 29 (2008) 601.
- [12] J.F. DuMond, S.B. King, Antioxid. Redox Signal. 14 (2011) 1637.
- [13] A.C. Montenegro, V.T. Amorebieta, L.D. Slep, D.F. Martin, F. Roncaroli, D.H. Murgida, S.E. Bari, J.A. Olabe, Angew. Chem., Int. Ed. 48 (2009) 4213.
- [14] J.C. Toledo, H.A.S. Silva, M. Scarpellini, V. Mori, A.J. Camargo, M. Bertotti, D.W. Franco, Eur. J. Inorg. Chem. (2004) 1879.
- [15] E. Tfouni, M. Krieger, B.R. McGarvey, D.W. Franco, Coord. Chem. Rev. 236 (2003) 57.
- [16] E. Tfouni, F.G. Doro, L.E. Figueiredo, J.C.M. Pereira, G. Metzker, D.W. Franco, Curr. Med. Chem. 17 (2010) 3643.
- [17] J.C.M. Pereira, V. Carregaro, D.L. Costa, J.S. Silva, F.Q. Cunha, D.W. Franco, Eur. J. Med. Chem. 45 (2010) 4180.
- [18] D.D. Perrin, W.L.F. Armarego, D.R. Perrin, Purification of Laboratory Chemicals, Pergamon Press, Elmsford, 1980.
- [19] D.F. Shriver, The Manipulation of Air-Sensitive Compound, McGraw-Hill, New York, 1969.
- [20] L.H. Vogt, J.L. Katz, S.E. Wiberley, Inorg. Chem. 4 (1965) 1157.
- [21] L.G.F. Lopes, E.E. Castellano, A.G. Ferreira, C.U. Davanzo, M.J. Clarke, D.W. Franco, Inorg. Chim. Acta 359 (2005) 2883.
- [22] A.D. Ostrowski, S.J. Deakin, B. Azhar, T.W. Miller, N. Franco, M.M. Cherney, A.J. Lee, J.N. Burstin, J.M. Fukuto, I.L. Megson, P.C. Ford, J. Med. Chem. 53 (2010) 715.
- [23] G. Metzker, J.C. Toledo, F.C.A. Lima, A. Magalhães, D.R. Cardoso, D.W. Franco, J. Braz. Chem. Soc. 21 (2010) 1266.
- [24] M. Lovric, S. Komorsky-Lovric, J. Electroanal. Chem. 248 (1988) 239.
- [25] M.J. Frisch, G.W. Trucks, H.B. Schlegel, G.E. Scuseria, M.A. Robb, J.R. Cheeseman, J.A. Montgomery Jr., T. Vreven, K.N. Kudin, J.C. Burant, J.M. Millam, S. S. Iyengar, J. Tomasi, V. Barone, B. Mennucci, M. Cossi, G. Scalmani, N. Rega, G.A. Petersson, H. Nakatsuji, M. Hada, M. Ehara, K. Toyota, R. Fukuda, J. Hasegawa, M. Ishida, T. Nakajima, Y. Honda, O. Kitao, H. Nakai, M. Klene, X. Li, J.E. Knox, H.P. Hratchian, J.B. Cross, V. Bakken, C. Adamo, J. Jaramillo, R. Gomperts, R.E. Stratmann, O. Yazyev, A.J. Austin, R. Cammi, C. Pomelli, J.W. Ochterski, P.Y. Ayala, K. Morokuma, G.A. Voth, P. Salvador, J.J. Dannenberg, V.G. Zakrzewski, S. Dapprich, A.D. Daniels, M.C. Strain, O. Farkas, D.K. Malick, A.D. Rabuck, K. Raghavachari, J.B. Foresman, J.V. Ortiz, Q. Cui, A.G. Baboul, S. Clifford, J. Cioslowski, B. B. Stefanov, G. Liu, A. Liashenko, P. Piskorz, I. Komaromi, R.L. Martin, D.J. Fox, T. Keith, M.A. Al-Laham, C.Y. Peng, A. Nanayakkara, M. Challacombe, P.M.W. Gill, B. Johnson, W. Chen, M.W. Wong, C. Gonzalez, J.A. Pople, Gaussian, Inc., Wallingford, CT, 2004.
- [26] W. Kohn, L.J. Sham, Phys. Rev. 140 (1965) A1133.
- [27] C. Lee, W. Yang, R.G. Parr, Phys. Rev. B 37 (1988) 785.
- [28] A.D. Becke, J. Chem. Phys. 98 (1993) 5648.
- [29] P.J. Hay, W.R. Wadt, J. Chem. Phys. 82 (1985) 270.
- [30] W.R. Wadt, P.J. Hay, J. Chem. Phys. 82 (1985) 284.
- [31] P.J. Hay, W.R. Wadt, J. Chem. Phys. 82 (1985) 299.
- [32] E.D. Glendenning, J.K. Badenhop, A.E. Reed, J.E. Carpenter, J.A. Bohmann, C.M. Morales, F. Wehold, NBO 3.0, Theoretical Chemistry Institute, University of Wisconsin, Madison, 2001.
- [33] E. Cancès, B. Mennucci, J. Tomasi, J. Chem. Phys. 107 (1997) 3032.
- [34] A.E. Reed, F. Wehold, J. Chem. Phys. 83 (1985) 1736.
- [35] A.E. Reed, L.A. Curtiss, F. Wehold, Chem. Rev. 88 (1988) 899.
- [36] C.G. Pierpont, D.G. Van Derveer, W. Durland, R. Eisenberg, J. Am. Chem. Soc. 92 (1970) 4760.
- [37] M.D. Bartberger, W. Liu, E. Ford, K.M. Miranda, C. Switzer, J.M. Fukuto, P.J. Farmer, D.A. Wink, K.N. Houk, Proc. Natl. Acad. Sci. USA 99 (2002) 10958.
- [38] V. Shafirovich, S.V. Lymar, Proc. Natl. Acad. Sci. USA 99 (2002) 7340.
- [39] C. Gossens, A. Dorcier, P.J. Dyson, U. Rothlisberg, Organometallics 26 (2007) 3969.
- [40] M.D. Liptak, G.C. Shields, J. Am. Chem. Soc. 123 (2001) 7314.
- [41] R.B. Peters, D.G. Fischer, Quantitative Chemical Analysis, W.B. Saunders Company, Philadelphia, 1969.
- [42] N.S. Hush, J. Blackledge, J. Electroanal. Chem. 5 (1963) 420.
- [43] F.A. Cotton, G. Wilkinson, C.A. Murillo, M. Bochmann, Advanced Inorganic Chemistry, Wiley-Interscience, New York, 1999.
- [44] B. Wang, X. Li, Anal. Chem. 70 (1998) 2181.
- [45] D.W. Franco, H. Taube, Inorg. Chem. 17 (1978) 571.
- [46] F. Roncaroli, J.A. Olabe, Inorg. Chem. 44 (2005) 4719.
- [47] Y. Chen, F.T. Lin, R.E. Shepherd, Inorg. Chem. 38 (1999) 973.
- [48] C.C. Golfeto, G. Von Poelhsitz, H.S. Selistre-de-Araújo, M.P. Araujo, J. Ellena, E.E. Castellano, L.G.L. Lopes, I.S. Moreira, A.A. Batista, J. Inorg. Biochem. 104 (2010) 489.
- [49] D.R. Truzzi, A.G. Ferreira, S.C. Silva, E.E. Castellano, F.C.A. Lima, D.W. Franco, Dalton Trans. 40 (2011) 12917.